# Dalton Transactions

Accepted Manuscript






ROYAL SOCIETY OF CHEMISTRY

www.rsc.org/dalton

# Novel reactions of homodinuclear $Ni_2$ complexes $[Ni(RN_{Py}S_4)]_2$ with $Fe_3(CO)_{12}$ to give heterotrinuclear $NiFe_2$ and mononuclear Fe complexes relevant to [NiFe]- and [Fe]-hydrogenases†

**Li-Cheng Song,* Meng Cao and Yong-Xiang Wang**

The homodinuclear complexes $[Ni(RN_{Py}S_4)]_2$ (**1a–1e**; $RN_{Py}S_4$ = 2,6-bis(2-mercaptophenylthiomethyl)-4-R-pyridine; R = H, MeO, Cl, Br, *i*-Pr) were found to be prepared by reactions of the in situ generated $Li_2[Ni(1,2\text{-}S_2C_6H_4)_2]$ with 2,6-bis[(tosyloxy)methyl]pyridine and its substituted derivatives 2,6-bis[(tosyloxy)methyl]-4-R-pyridine. Further reactions of **1a–1e** with $Fe_3(CO)_{12}$ gave both heterotrinuclear complexes $NiFe_2(RN_{Py}S_4)(CO)_5$ (**2a–2e**) and mononuclear complexes $Fe(RN_{Py}S_4)(CO)$ (**3a–3e**), unexpectedly. Interestingly, complexes **2a–2e** and **3a–3e** could be regarded as models for the active sites of [NiFe]- and [Fe]-hydrogenases, respectively. All the prepared complexes were characterized by elemental analysis, spectroscopy, and particularly for some of them by X-ray crystallography. In addition, the electrochemical properties of **2a–2e** and **3a–3e** as well as the electrocatalytic $H_2$ production catalyzed by **2a–2e** and **3a–3e** were investigated by CV techniques.

*Department of Chemistry, State Key Laboratory of Elemento-Organic Chemistry, Collaborative Innovation Center of Chemical Science and Engineering (Tianjin), Nankai University, Tianjin 300071, China. E-mail: lcsong@nankai.edu.cn.*

† Electronic supplementary information (ESI) available: Preparation of 2,6-bis[(tosyloxy)methyl]-4-*i*-propylpyridine, thermal decomposition experiments of trinuclear complexes **2a-2e**, overpotential determinations for **2a-2e** and **3a-3e**, cyclic voltammograms of **2b-2e** and **3b-3e** with TFA, Tables S1/S2 and Figures S1-S9. CCDC reference numbers 1015684-1015688. For crystallographic data in CIF see DOI: 10.1039/b000000x/.

**Introduction**

Hydrogenases are a class of highly efficient enzymes that catalyze the hydrogen metabolism in a variety of microorganisms, such as archaea, bacteria, and some eukaryotes.[1-4] According to the metal content in their active sites, hydrogenases can be mainly classified as three families, namely [FeFe]-hydrogenases,[5-7] [NiFe]-hydrogenases,[8-10] and [Fe]-hydrogenase (Hmd).[11-13] Among the three phylogenetically different enzymes, [NiFe]- and [FeFe]-hydrogenases are redox-active enzymes that can catalyze the reversible redox reaction between molecular $H_2$ and protons,[5-10] but [Fe]-hydrogenase is not redox-active enzyme that catalyzes the reversible hydride transfer from molecular $H_2$ to its substrate methenyltetrahydromethanopterin (methenyl-$H_4$MPT$^+$) to give methylenetetrahydromethanopterin (methylene-$H_4$MPT) and $H^+$.[11-13] X-ray crystallographic study revealed that the active site of [NiFe]-hydrogenases contains two metal centers, in which Ni center is coordinated by two terminal cysteine Cys–S ligands and Fe center is coordinated by one terminal CO and two terminal $CN^-$ ligands, as well as the two metal centers are combined together by two bridging Cys–S ligands (Figure 1a).[14-18] However, in contrast to [NiFe]-hydrogenases, the active site of [Fe]-hydrogenase contains only a single Fe center that is coordinated by two *cis*-carbonyl ligands, one cysteine S atom, one $\eta^2$-acymethylpyridinol ligand, and one as yet unknown ligand, which is presumably a water molecule (Figure 1b).[12,19,20]

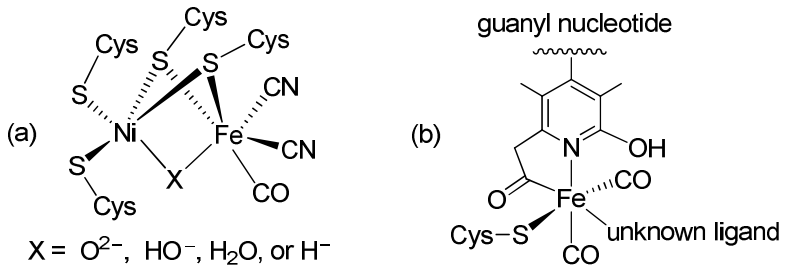


**Fig. 1** (a) Active site of [NiFe]-hydrogenases. (b) Active site of [Fe]-hydrogenase.

Guided by the well-elucidated active site structures of [NiFe]- and [Fe]-hydrogenases, synthetic chemists have designed and synthesized many transition-metal complexes as models for the active sites of [NiFe]-hydrogenases[21-42] and [Fe]-hydrogenase.[20,43-53] Recently, we launched a study on reactions of $Fe_3(CO)_{12}$ with the $[RN_{Py}S_4]$-type ligand-containing homodinuclear $Ni_2$ complexes $[Ni(RN_{Py}S_4)]_2$ ($RN_{Py}S_4$ = 2,6-bis(mercaptophenylthiomethyl)-4-R-pyridine; R = H,[54] MeO, Cl, Br, *i*-Pr), aimed to prepare the new type of $[Ni(RN_{Py}S_4)]$ unit-containing [NiFe]-hydrogenase model complexes. This is because such model complexes are expected to be more stable than those $[NiS_4]$ unit-containing model complexes[30,33] due to one additional coordination of the pyridine N atoms to their Ni atoms. In addition, the presence of R substituents on their pyridine rings may allow one to study the influence of the $[RN_{Py}S_4]$-type ligand upon the structures and properties of such a new type of [NiFe]-hydrogenase model complexes. However, to our surprise, the reactions gave not only the $[RN_{Py}S_4]$-type ligand-containing heterotrinuclear [NiFe]-hydrogenase model complexes, but also afforded the $[RN_{Py}S_4]$-type ligand-containing mononuclear [Fe]-hydrogenase model complexes. In this article, we report the synthesis and structures of the $[RN_{Py}S_4]$ (R = H, MeO, Cl, Br, *i*-Pr)-type

ligand-containing trinuclear $NiFe_2$ and mononuclear Fe model complexes along with their starting dinuclear $Ni_2$ complexes. In addition, the electrochemical properties of the [NiFe]- and [Fe]-hydrogenase model complexes, as well as their electrocatalytic $H_2$ producing ability are also described.

## Results and discussion

### Synthesis and characterization of homodinuclear complexes $[Ni(RN_{Py}S_4)]_2$ (1a-1e)

It was found that treatment of 1,2-benzenedithiol with MeOLi followed by coordination reaction of $1,2\text{-}(LiS)_2C_6H_4$ with $Ni(OAc)_2{\cdot}4H_2O$ gave rise to mononuclear Ni complex $Li_2[Ni(1,2\text{-}S_2C_6H_4)_2]$; further nucleophilic substitution reaction of this mononuclear Ni complex with 2,6-bis[(tosyloxy)methyl]pyridine[54] or reactions with its substituted derivatives 2,6-bis[(tosyloxy)methyl]-4-R-pyridine (R = MeO, Cl, Br, *i*-Pr) and subsequent dimerization resulted in formation of the homodinuclear complexes $[Ni(RN_{Py}S_4)]_2$ **(1a-1e)** in 41−73% yields (Scheme 1).

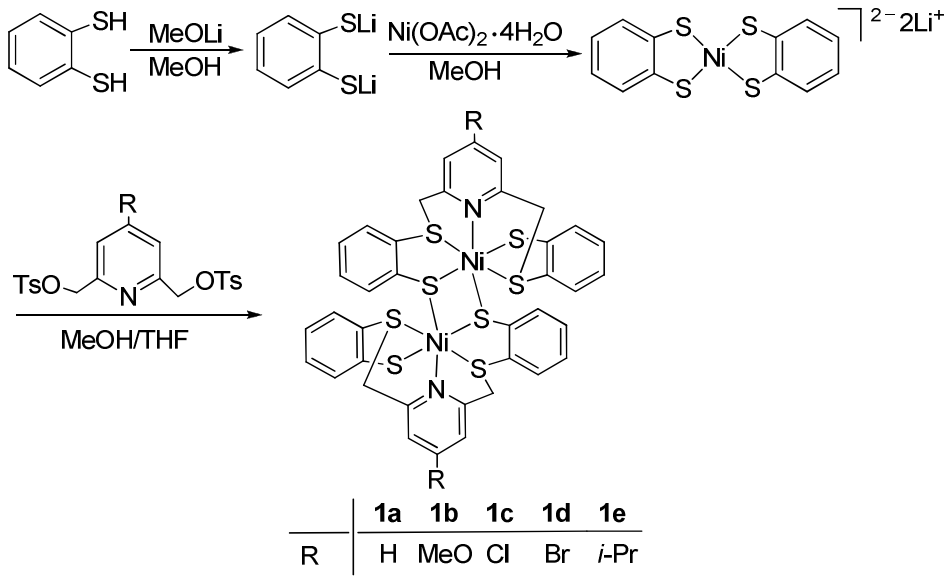


**Scheme 1** Synthesis of complexes **1a-1e**.

Complexes **1a-1e** are air-stable brown solids. While **1a-1d** do not dissolve in THF, $CH_2Cl_2$, MeOH, and $Et_2O$, **1e** is readily soluble in THF and $CH_2Cl_2$, slightly soluble in MeOH, and insoluble in $Et_2O$ and hexane. Among complexes **1a-1e**, only **1a** was previously reported by Sellmann and co-workers.[54] The elemental analysis indicated that each of **1a-1d** contains one molecule of MeOH, but **1e** does not contain MeOH, obviously due to its purification by recrystallization from a mixed solvent $CH_2Cl_2$/hexane. In addition, the mass spectra of **1a–1e** showed their molecular ion peaks. It should be noted that we were unable to determine the solution $^1$H NMR spectra of **1a –1d** since they are not soluble in the common deuterioorganic solvents. In addition, although **1e** is soluble in the common deutereoorganic solvents, its solution $^1$H NMR spectrum was also unable to be determined due to its paramagnetic property. The magnetic moment of **1e** was determined by Evans method[55] to give a $\mu_{eff}$ value of 2.84 $\mu_B$ at 290 K. This value is less than the corresponding value for

parent complex **1a** (3.28 $\mu_B$).[54]

Fortunately, the molecular structure of complex **1e** was unequivocally confirmed by X-ray crystal diffraction analysis (Figure 2, Table 1). As shown in Figure 2, complex **1e** is indeed a dimer that consists of two identical [Ni(*i*-PrN$_{Py}$S$_4$)] units in which both Ni1 and Ni1A centers have a pseudo-octahedral geometry. In one [Ni(*i*-PrN$_{Py}$S$_4$)] unit the Ni1 center is coordinated by thiolate S1/S3 and thioether S2, S4/S4A atoms, and pyridine N1 atom, while in another [Ni(*i*-PrN$_{Py}$S$_4$)] unit the Ni1A center is coordinated by thiolate S1A/S3A and thioether S2A, S4A/S4 atoms and pyridine N1A atom. Complex **1e** possesses $C_2$ symmetric property and its two Ni–N bond lengths (Ni1–N1 = Ni1A–N1A = 2.087 Å) are very close to those of its parent complex **1a (**Ni1–N1 = Ni1A–N1A = 2.060 Å).[54]

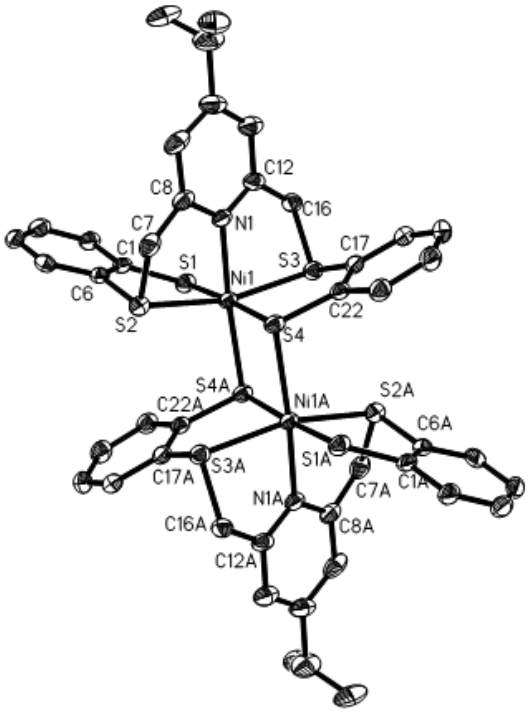


**Fig. 2** Molecular structure of **1e** with 30% probability level ellipsoids.

**Table 1** Selected bond lengths (Å) and angles (°) for **1e**

| | | | |
|---|---|---|---|
| Ni(1)-N(1) | 2.087(3) | Ni(1)-S(1) | 2.3631(12) |
| Ni(1)-S(4) | 2.3812(11) | Ni(1)-S(2) | 2.3868(13) |
| S(4)-Ni(1A) | 2.4409(11) | Ni(1)-S(3) | 2.4039(13) |
| N(1)-Ni(1)-S(1) | 91.30(10) | N(1)-Ni(1)-S(4) | 91.89(10) |
| S(1)-Ni(1)-S(4) | 176.78(4) | N(1)-Ni(1)-S(2) | 82.76(11) |
| Ni(1)-S(4)-Ni(1A) | 95.28(4) | S(4)-Ni(1)-S(4A) | 84.71(4) |

**Synthesis and characterization of heterotrinuclear complexes $NiFe_2(RN_{Py}S_4)(CO)_5$ (2a-2e) and mononuclear complexes $Fe(RN_{Py}S_4)(CO)$ (3a-3e)**

Initially, we found that when a suspension of parent homodinuclear complex $[Ni(RN_{Py}S_4)]_2$ (**1a**, R = H) was treated with $Fe_3(CO)_{12}$ in $CH_2Cl_2$ at room temperature for 12 h, nearly 93% of **1a** was recovered without any isolable product. However, in contrast to this, when the suspension of **1a** was treated with $Fe_3(CO)_{12}$ in refluxing $CH_2Cl_2$ for 12 h, both heterotrinuclear complex $NiFe_2(RN_{Py}S_4)(CO)_5$ (**2a**, R = H) and mononuclear complex $Fe(RN_{Py}S_4)(CO)$ (**3a**, R = H) were unexpectedly obtained in 23% and 41% yields, respectively (Scheme 2).

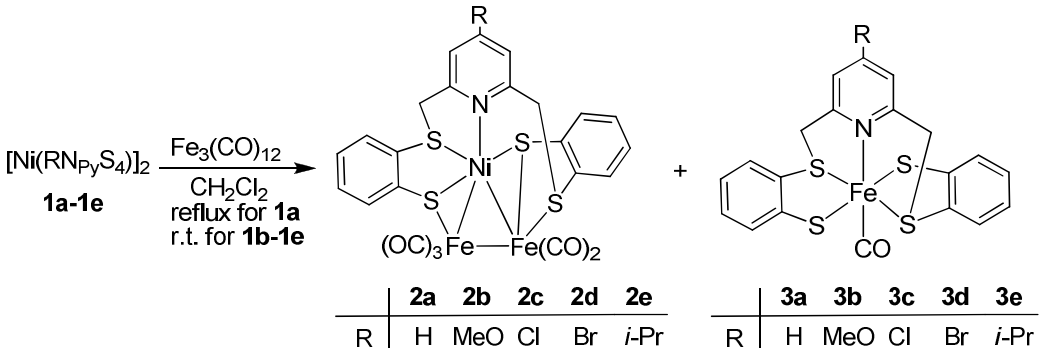


**Scheme 2** Synthesis of complexes **2a-2e** and **3a-3e**.

To examine the influence of R substituents in dinuclear complexes $[Ni(RN_{Py}S_4)]_2$ and to show the generality of this novel type of reactions, we continued to try

reactions of the suspensions of the substituted dinuclear complexes **1b-1d** and the solution of **1e** in $CH_2Cl_2$ with $Fe_3(CO)_{12}$ at room temperature. As a result, the corresponding trinuclear complexes **2b–2e** and mononuclear complexes **3b–3e** were produced simultaneously in 15%–28% and 17%–53% yields, respectively (Scheme 2). It follows that (i) this type of reactions are quite general for producing both trinuclear $NiFe_2(RN_{Py}S_4)(CO)_5$ and mononuclear $Fe(RN_{Py}S_4)(CO)$ complexes in $CH_2Cl_2$, regardless of the dinuclear complexes $[Ni(RN_{Py}S_4)]_2$ being parent (**1a**, R = H) or substituted (**1b-1e**, R = MeO, Cl, Br, *i*-Pr); and (ii) the chemical reactivity of the substituted dinuclear complexes **1b-1e** is much higher than that of their parent complex **1a**, regardless of the substituents being electron-donating or electron-withdrawing.

At the present stage, we are not clear about the whole reaction pathway and the mechanistic details for production of **2a**–**2e** and **3a**–**3e**. However, the trinuclear $NiFe_2$ complexes **2a**–**2e** might be formally regarded as produced by reaction of monomers $Ni(RN_{py}S_4)$ with fragment $Fe_2(CO)_8$, both generated in situ from thermal decomposition of the starting materials $[Ni(RN_{py}S_4)]_2$ and $Fe_3(CO)_{12}$. In addition, the mononuclear Fe(+II) complexes **3a**–**3e** could be considered as produced in situ by the thermally oxidative decomposition of the initially formed trinuclear [Ni(+II)2Fe(0)] complexes **2a**–**2e**, through which the Fe(0) centers of **2a**–**2e** were oxidized by their Ni(+II) centers to give the Fe(+II) centers of **3a**–**3e**. This is because when the parent trinuclear complex **2a** was stirred under $N_2$ in refluxing $CH_2Cl_2$ for 12 h, or when the substituted trinuclear complexes **2b**–**2e** were stirred under $N_2$ in $CH_2Cl_2$ at room

temperature for 12 h, after column chromatographic separation under anaerobic conditions, the corresponding mononuclear complexes **3a**–**3e** were obtained in 11-21% yields (see the Supporting Information).

Complexes **2a**–**2e** and **3a**–**3e** are air-stable brown-red or red solids, which are easily soluble in $CH_2Cl_2$ and THF, sparingly soluble in $Et_2O$, and insoluble in hexane. Among these complexes, only **3a** was previously prepared by another method.[54] Complexes **2a**–**2e** and **3a**–**3e** prepared by us have been fully characterized by elemental analysis and various spectroscopic methods. The IR spectra of **2a**–**2e** displayed three to five strong absorption bands in the range 1999–1890 $cm^{-1}$ for their five terminal carbonyls, whereas **3a**–**3e** exhibited only one very strong band in the region 1968–1957 $cm^{-1}$ for their one terminal carbonyls. The $^1H$ NMR spectra of **2a**–**2e** showed two doublets at the higher field from 4.46 to 4.82 ppm for their $NiSCH_2$ protons and two doublets at the lower field from 4.83 to 5.08 ppm for their $FeSCH_2$ protons. Such $^1H$ NMR assignments are reasonable since the mononuclear Fe complexes **3a-3e** displayed two doublets at the lower field from 4.77 to 5.02 ppm for their $SCH_2$ groups attached to Fe atoms. In addition, the $^{13}C\{^1H\}$ NMR spectra of **2a-2e** exhibited three signals in the region 212–224 ppm for their five terminal carbonyls, whereas **3a-3e** showed only one signal in the range 215–219 ppm for their one terminal carbonyl ligands.

The molecular structures of trinuclear complexes **2a** and **2b** were further confirmed by X-ray crystallography. Figure 3 and Figure S1 show their molecular structures. Table 2 and Table S1 list their selected bond lengths and angles. Since **2a**

and **2b** are basically isostructural, we just discuss the molecular structure of **2a**. As shown in Figure 3, the Ni1 center of **2a** is coordinated by thioether S3 atom, thiolate S2/S4 atoms, and pyridine N1 atom to form a mononuclear Ni moiety Ni($HN_{Py}S_4$), which is linked to an $Fe_2(CO)_5$ unit via the metal-metal bonds Ni1–Fe1/Ni1–Fe2 and metal-sulfur bonds Fe1-S1/Fe1-S2/Fe2-S4. The three metal centers Fe1/Fe2/Ni1 all adopt a pseudo-octahedral geometry and the Ni-Fe bond lengths of **2a** (Ni1–Fe1 = 2.4484 Å, Ni1–Fe2 = 2.4825 Å) are just slightly shorter than those (2.5–2.6 Å) found in the reduced form of [NiFe]-hydrogenases.[16,18] In addition, it should be noted that both **2a** and **2b** are the first examples of the unsymmetrical cluster core [$NiFe_2NS_4$]-containing [NiFe]-hydrogenase model complexes characterized by X-ray crystallography, although the symmetrical cluster core [$NiFe_2S_4$]-containing model complexes for [NiFe]-hydrogenases were previously crystallographically characterized.[30,33]

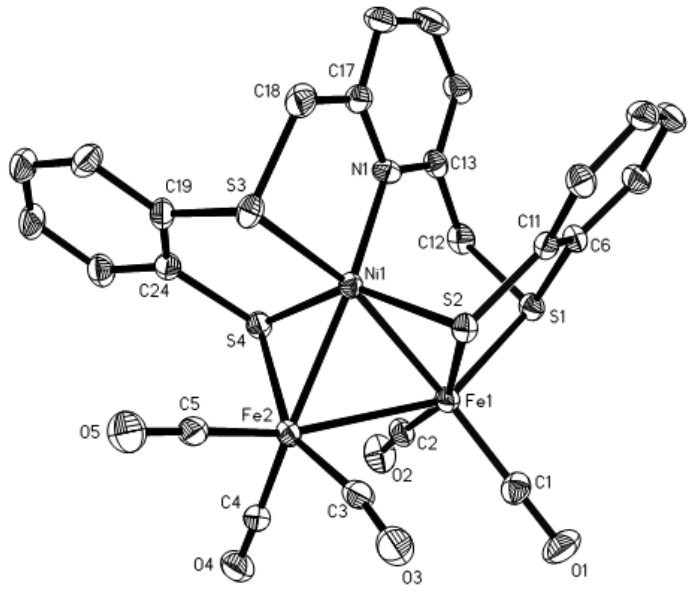


**Fig. 3** Molecular structure of **2a** with 30% probability level ellipsoids.

**Table 2** Selected bond lengths (Å) and angles (°) for **2a**

| | | | |
|---|---|---|---|
| Ni(1)-N(1) | 2.033(8) | Ni(1)-S(2) | 2.202(3) |
| Ni(1)-S(3) | 2.249(3) | Ni(1)-Fe(1) | 2.4484(19) |
| Ni(1)-Fe(2) | 2.4825(19) | Fe(1)-Fe(2) | 2.614(2) |
| Fe(1)-S(2) | 2.242(3) | Fe(2)-S(4) | 2.269(3) |
| N(1)-Ni(1)-Fe(1) | 112.7(2) | S(3)-Ni(1)-Fe(1) | 156.74(10) |
| S(2)-Ni(1)-Fe(1) | 57.35(8) | Ni(1)-Fe(1)-Fe(2) | 58.62(6) |
| Fe(1)-Ni(1)-Fe(2) | 64.03(6) | Fe(1)-Fe(2)-S(4) | 85.52(9) |
| Ni(1)-Fe(2)-Fe(1) | 57.35(5) | Fe(2)-Fe(1)-S(2) | 87.08(8) |

The molecular structures of mononuclear complexes **3b** and **3c** were also confirmed by X-ray crystallography. While their structures are shown in Figure 4 and Figure S2, Table 3 and Table S2 list their selected bond lengths and angles. As can be seen in Figure 4 and Figure S2, complexes **3b** and **3c** are structurally similar to the active site of [Fe]-hydrogenase (Figure 1b) and thus they can be regarded as structural models of [Fe]-hydrogenase. Both **3b** and **3c** contain only one iron (Fe1) center that is coordinated by a 4-substituted pyridine N1 atom, two thioether S2/S3 atoms, two thiolate S1/S4 atoms, and one terminal carbonyl ligand. The Fe–N bond lengths of **3b** (Fe1–N1 = 2.0128 Å) and **3c** (Fe1–N1 = 1.9972 Å ) are very close to that (Fe1–N1 = 2.014 Å) of their parent complex **3a**.[54] Particularly noteworthy is that the coordination manner of the terminal carbonyl ligand C21O2 in **3b** or C1O1 in **3c** is *trans* to the pyridine nitrogen atom, which is identical with that of one of the two terminal carbonyls present in the active site of [Fe]-hydrogenase.[12,19,20] In addition, the Fe1–N1 bond length of **3b** (2.0128 Å) or **3c** (1.9972 Å) is almost identical with that (2.006 Å) found in the natural [Fe]-hydrogenase.[20]

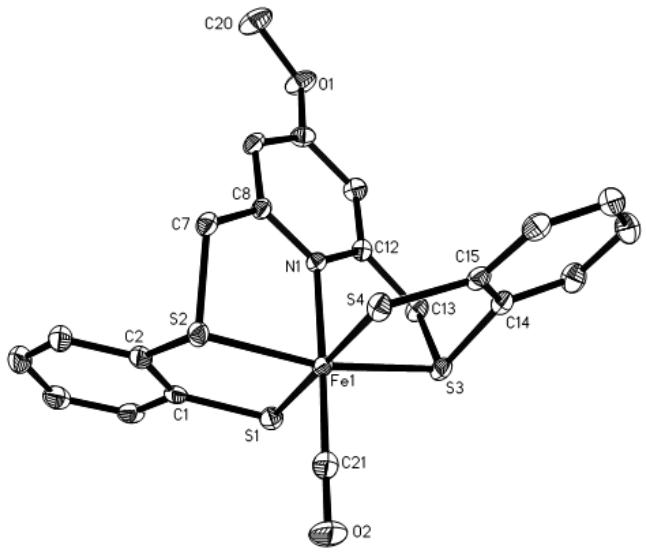


**Fig. 4** Molecular structure of **3b** with 30% probability level ellipsoids.

**Table 3** Selected bond lengths (Å) and angles (°) for **3b**

| | | | |
|---|---|---|---|
| Fe(1)-N(1) | 2.0128(13) | Fe(1)-S(2) | 2.2285(5) |
| Fe(1)-S(3) | 2.2342(5) | Fe(1)-S(1) | 2.2979(5) |
| Fe(1)-S(4) | 2.3028(5) | O(2)-C(21) | 1.148(2) |
| C(21)-Fe(1)-S(2) | 96.15(6) | C(21)-Fe(1)-S(3) | 96.50(6) |
| S(2)-Fe(1)-S(3) | 167.280(18) | S(1)-Fe(1)-S(4) | 179.302(18) |
| S(7)-Fe(2)-S(6) | 170.611(17) | S(5)-Fe(2)-S(8) | 178.670(18) |

**Electrochemical properties of 2a-2e and electrocatalytic $H_2$ production catalyzed by 2a-2e**

So far, the electrochemical and electrocatalytic properties of some [NiFe]-hydrogenase model complexes have been well-studied by cyclic voltammetric (CV) techniques.[36,41,42,56,57] The electrochemical properties of our model complexes **2a-2e** were determined in MeCN with *n*-$Bu_4NPF_6$ as electrolyte by CV techniques. While their cyclic voltammograms are shown in Figure 5, Table 4 lists the corresponding electrochemical data. As shown in Figure 5 and Table 4, the five model

complexes each displayed one irreversible oxidation peak and two irreversible reduction peaks. In addition, compared to the redox potentials of parent complex **2a**, those of **2b** and **2e** are slightly shifted towards the negative direction, while **2c** and **2d** are slightly shifted towards the positive direction. Apparently, these are in good agreement with the facts that **2b** and **2e** contain the electron-donating MeO and *i*-Pr substituents; **2c** and **2d** contain the electron-withdrawing Cl and Br substituents, respectively. In addition, we proved that the plots of the peak current ($i_p$) versus the square root of the scan rate ($\nu^{1/2}$) for the first and second reduction peaks of **2a** are linear (Figure S3) and thus the two reduction processes are most likely diffusion-controlled.[58]

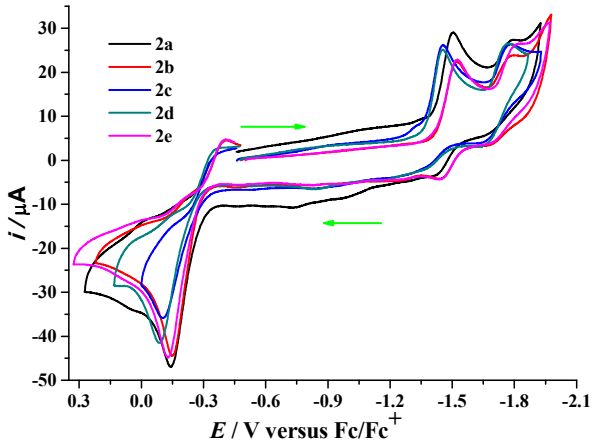


**Fig. 5** Cyclic voltammograms of **2a-2e** (1.0 mM) in 0.1 M *n*-$Bu_4NPF_6$/MeCN at a scan rate of 0.1 $Vs^{-1}$.

**Table 4** Electrochemical data of **2a-2e**[a]

| compound | $E_{pc1}$/V | $E_{pc2}$/V | $E_{pa}$/V |
|---|---|---|---|
| **2a** | −1.51 | −1.79 | −0.14 |
| **2b** | −1.52 | −1.80 | −0.15 |
| **2c** | −1.46 | −1.77 | −0.08 |

| | | | |
|---|---|---|---|
| **2d** | −1.45 | −1.77 | −0.07 |
| **2e** | −1.53 | −1.82 | −0.15 |

[a] All potentials are versus $Fc/Fc^+$ in 0.1 M *n*-$Bu_4NPF_6$/MeCN at a scan rate of 0.1 $Vs^{-1}$.

To examine whether complexes **2a–2e** can catalyze proton reduction to hydrogen, we further determined their cyclic voltammograms in the presence of various amounts of trifluoroacetic acid (TFA). As shown in Figure 6 and Figure S4 (see the Supporting Information), when TFA was sequentially added from 2 mM to 10 mM, the current heights of the original two reduction peaks of **2a–2e** were both obviously increased, and particularly the current heights of the original second reduction peaks of **2a–2e** were increased more rapidly than those of the first reduction peaks. Apparently, such an observation indicated that the $H_2$ production from TFA catalyzed by **2a–2e** occurred around their original first and second reduction potentials.[59] To further confirm the $H_2$ production, we carried out the bulk electrolysis of a MeCN solution of **2a–2e** (0.5 mM) with excess TFA (15 mM). The average turnover numbers (TONs) and turnover frequencies (TOFs) determined during 0.5 h of the bulk electrolysis are listed in Table 5. Obviously, the TON and TOF values for **2a–2e** are much higher than those previously reported for the $H_2$ production from TFA catalyzed by [NiFe]-hydrogenese model complex $NiFe_2(MeC_6H_3S_2)_2(CH_2)_3(CO)_6$[60] (TON = 6, TOF = 6/h) and Lubitz model complex [Ni(xbsms)(μ-CO)(μ-S)($Fe(CO)_2$(′S)′]($H_2$xsms=1,2-bis(4-mercapto-3,3′-dimethyl-2-thiobutyl)benzene) (TON = 20, TOF = 5/h).[61] In addition, the overpotentials for **2a–2e** in MeCN with TFA were also obtained using Evans′ relationship[61,62] (see Table 5 and

Figures S5/S6 in the Supporting Information), which are slightly lower than that (540 mV) for the aforementioned Lubitz complex. It should be noted that the overpotential, TON and TOF for parent complex **2a** are slightly higher than the corresponding those for the substituted complexes **2b–2e**, irrespective of the substituents being electron-donating or electron-withdrawing. In addition, the gas chromatographic (GC) analysis showed that the yields of $H_2$ produced during the bulk electrolysis in the presence of **2a–2e** are above 90%.

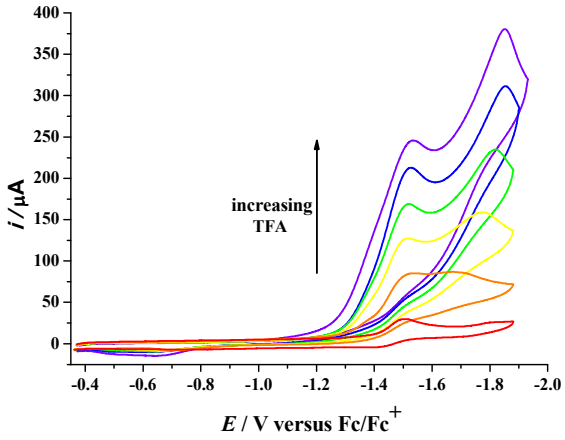


**Fig. 6** Cyclic voltammograms of **2a** (1.0 mM) with TFA (0, 2, 4, 6, 8, 10 mM) in 0.1 M *n*-$Bu_4NPF_6$/MeCN at a scan rate of 0.1 $Vs^{-1}$.

**Table 5.** Electrocatalytic data of **2a-2e**[a]

| compound | overpotential/mV | TON | TOF/$h^{-1}$ |
|---|---|---|---|
| **2a** | 525 | 23[b] | 46 |
| **2b** | 520 | 20[c] | 40 |
| **2c** | 490 | 21[d] | 42 |
| **2d** | 515 | 21[e] | 42 |
| **2e** | 505 | 20[f] | 40 |

[a] Overpotential, TON and TOF for **2a-2e** were determined by the same methods, respectively. [b] Determined at –1.90 V. [c] Determined at –1.92 V. [d] Determined at –1.85 V. [e] Determined at –1.86 V. [f] Determined at –1.91 V.

**Electrochemical properties of 3a–3e and electrocatalytic $H_2$ production catalyzed by 3a–3e.**

Although the electrochemical and electrocatalytic properties of a large number of [FeFe]-hydrogenase model complexes have been extensively studied,[63-65] the [Fe]-hydrogenase model complexes are much less investigated, both electrochemically and electrocatalytically.[51,66,67] The electrochemical properties of our model complexes **3a–3e** were also investigated in MeCN with *n*-$Bu_4PF_6$ as the electrolyte by CV techniques. Figure 7 shows their cyclic voltammograms, whereas the corresponding electrochemical data are given in Table 6. As shown in Figure 7 and Table 6, the five complexes exhibited one quasi-reversible oxidation peak and one irreversible reduction peak. Similar to the case for [NiFe]-hydrogenase model complexes **2a-2e**, the redox potentials of the substituted [Fe]-hydrogenase model complexes **3b** and **3e** are slightly shifted towards the negative direction relative to that of their parent complex **3a**, whereas **3c** and **3d** are slightly shifted towards the positive direction. These are also in good agreement with the facts that **3b** and **3e** have the electron-donating MeO and *i*-Pr substituents; **3c** and **3d** have the electron-withdrawing Cl and Br substituents, respectively. In addition, similar to the case of trinuclear complex **2a**, the reduction process of mononuclear complex **3a** is also diffusion-controlled since the plot of the peak current ($i_p$) versus the square root of the scan rate ($\nu^{1/2}$) for the reduction peak of **3a** is linear (Figure S7).[58]

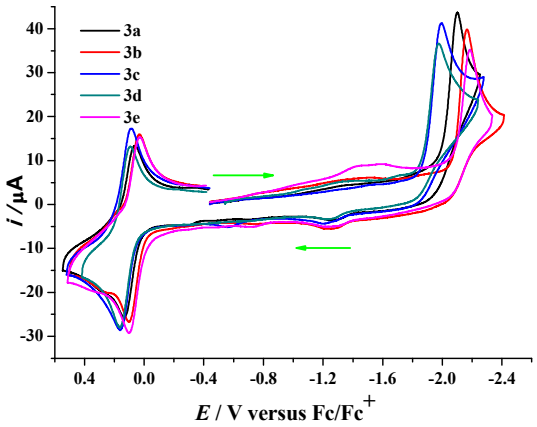


**Fig. 7** Cyclic voltammograms of **3a-3e** (1.0 mM) in 0.1 M *n*-$Bu_4NPF_6$/MeCN at a scan rate of 0.1 $Vs^{-1}$.

**Table 6.** Electrochemical data of **3a-3e**[a]

| compound | $E_{pc}$/V | $E_{pa}$/V ($\Delta E_p$/mV, $i_c/i_a$) |
|---|---|---|
| **3a** | –2.09 | 0.14 (70, 0.7) |
| **3b** | –2.16 | 0.10 (71, 0.7) |
| **3c** | –1.99 | 0.16 (76, 0.7) |
| **3d** | –1.98 | 0.16 (69, 0.7) |
| **3e** | –2.17 | 0.10 (70, 0.7) |

[a] All potentials are versus $Fc/Fc^+$ in 0.1 M *n*-$Bu_4NPF_6$/MeCN at a scan rate of 0.1 $Vs^{-1}$.

To date, only a few of the [Fe]-hydrogenase model complexes have been found to have the catalytic function for proton reduction to hydrogen[51,67] (although it does not belong to the catalytic function of the natural enzyme [Fe]-hydrogenase). Now, we have further found that **3a–3e** are also the electrocatalysts for proton reduction to hydrogen. The electrocatalytic behavior of **3a–3e** were studied by CV techniques in the presence of TFA (0–10 mM) in MeCN. As can be seen in Figure 8 and Figure S8 (see the Supporting Information), when the first 2 mM of TFA was added to **3a–3e**, a new reduction peak appeared from –1.67 to –1.80 V. In addition, the current heights

of the first peaks and the original reduction peaks increased remarkably when the acid was continuously added. As mentioned above for the case of **2a–2e**, such remarkable increases of the acid-induced current heights could be attributed to the electrocatalytic proton reduction processes.[51,67] To further confirm the $H_2$ production catalyzed by **3a–3e**, we carried out the bulk electrolysis of a MeCN solution of **3a–3e** (0.5 mM) with excess TFA (15 mM). The average TONs and TOFs determined during 0.5 h of the bulk electrolysis are listed in Table 7. It is evident that the TON values for the catalytic $H_2$ production from TFA catalyzed by **3a–3e** are much higher than those catalyzed by the [Fe]-hydrogenase model complexes Fe(3,6-dichloro-1,2-benzenedithiolate)$(CO)_2(PMe_3)_2$ (TON = 8)[67] and 2-C(O)$CH_2$-6-Ph$CO_2CH_2C_5H_3N$]Fe$(CO)_2$(2-$SC_5H_4NS$) (TON = 14.5)[51] under similar conditions. The overpotentials for **3a–3e** in MeCN with TFA were obtained using Evans′ relationship[61,62] (see Table 7 and Figure S9 in the Supporting Information). Unfortunately, we cannot make a comparison of these overpotential values with some others since no such data were previously reported for the [Fe]-hydrogenase model complexes. It can be seen in Table 7 that (i) the overpotentials of the electron-withdrawing substituent-containing complexes **3c** and **3d** are much higher than those of parent complex **3a** and the electron-donating substituent-containing complexes **3b** and **3e**, and (ii) the TON and TOF values of the electron-withdrawing substituent-containing complexes **3c** and **3d** are slightly lower than those of parent complex **3a** and the electron-donating substituent-containing complexes **3b** and **3e**. It is worth pointing out that GC analysis indicated that the yields of $H_2$ evolved during

the bulk electrolysis in the presence of **3a–3e** are above 90%.

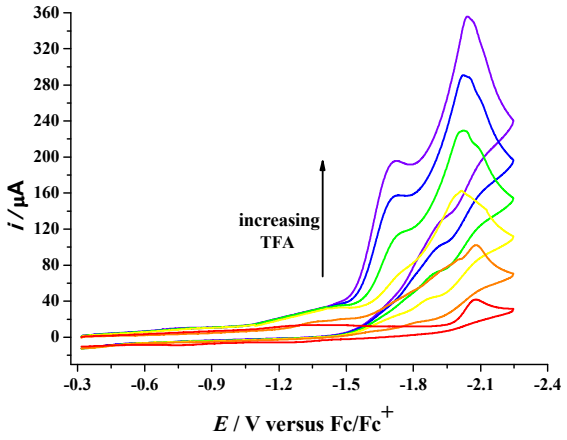


**Fig. 8** Cyclic voltammograms of **3a** (1.0 mM) with TFA (0, 2, 4, 6, 8, 10 mM) in 0.1 M *n*-$Bu_4NPF_6$/MeCN at a scan rate of 0.1 $Vs^{-1}$.

**Table 7.** Electrocatalytic data of **3a-3e**[a]

| compound | overpotential/mV | TON | TOF/$h^{-1}$ |
|---|---|---|---|
| **3a** | 670 | 20[b] | 40 |
| **3b** | 690 | 22[c] | 44 |
| **3c** | 750 | 15[d] | 30 |
| **3d** | 745 | 14[e] | 28 |
| **3e** | 670 | 21[f] | 42 |

[a] Overpotential, TON and TOF for **3a–3e** were determined by the same methods, respectively. [b] Determined at –2.15 V. [c] Determined at –2.15 V. [d] Determined at –1.90 V. [e] Determined at –1.90 V. [f] Determined at –2.15 V.

## Conclusions

We have found that the dinuclear $Ni_2$ complexes **1a-1e** can react with $Fe_3(CO)_{12}$ to give both trinuclear $NiFe_2$ complexes **2a-2e** and mononuclear Fe complexes **3a-3e** under mild conditions, unexpectedly. While all the prepared-complexes **1a-1e**, **2a-2e**, and **3a-3e** are characterized by elemental analysis and spectroscopy, the structures of **1e, 2a/2b**, and **3b/3c** are confirmed by X-ray crystallographic studies. The X-ray

crystallographic study on [NiFe]-hydrogenase model complexes **2a/2b** reveals that they indeed contain a heptadentate [$HN_{Py}S_4$] or [$(MeO)N_{Py}S_4$] ligand that is coordinated to a triangular $NiFe_2$ cluster core bearing five Fe-bound carbonyls; in addition, their metal Ni and Fe centers all adopt a pseudo-octahedral geometry. Different from model complexes **2a/2b**, the X-ray crystallographic study demonstrates that the [Fe]-hydrogenase model complexes **3b/3c** consist of a single Fe center that is ligated to one terminal CO ligand and a pentadentate [$(MeO)N_{Py}S_4$] or [$ClN_{Py}S_4$] ligand via one pyridine N atom and four thiolate/thioether S atoms; in addition, the terminal CO ligands in **3b/3c** are *trans* to their pyridine N atoms. The CV studies on [NiFe]- and [Fe]-hydrogenase model complexes **2a-2e** and **3a-3e** indicate that (i) the redox potentials of the substituted complexes **2b/2e** and **3b/3e** are slightly shifted towards the negative direction relative to those of their parent complexes **2a** and **3a**, respectively; (ii) the redox potentials of **2c/2d** and **3c/3d** are slightly shifted towards the positive direction relative to those of their parent complexes **2a** and **3a**, respectively; and (iii) such observations are completely consistent with the facts that **2b/2e** and **3b/3e** each have an electron-donating substituent; **2c/2d** and **3c/3d** each have an electron-withdrawing substituent. Finally, it should be noted that complexes **2a-2e** and **3a-3e** have been found to be electrocatalysts for TFA proton reduction to give hydrogen under CV conditions.

## Experimental section

### General comments

All reactions were carried out using standard Schlenk and vacuum-line techniques under an atmosphere of highly purified nitrogen. Dichloromethane was purified by distillation over $CaH_2$, absolute methanol from freshly prepared magnesium methoxide. Tetrahydrofuran, hexane, and diethyl ether were purified by distillation from a sodium benzophenone mixture. $Ni(OAc)_2{\cdot}4H_2O$, MeOLi (1 M in MeOH) were available commercially and used as received. 1,2-Benzenedithiol,[68] 2,6-bis[(tosyloxy)methyl]pyridine,[69] 2,6-bis [(tosyloxy)methyl]-4-methoxylpyridine,[69] 2,6-bis[(tosyloxy)methyl]- 4-chloropyridine,[69] 2,6-bis[(tosyloxy)methyl]-4-bromopyridine,[69] $Fe_3(CO)_{12}$,[70] were prepared according to the published procedures. IR spectra were recorded on a Bio-Rad FTS 135 and Bruker Tensor 27 FT-IR infrared spectrophotometers. $^1H$ and $^{13}C\{^1H\}$ NMR spectra were obtained on a Bruker Avance 400 NMR spectrometer. Elemental analyses were performed on an Elementar Vario EL analyzer. Mass spectra were determined on Finnigan lcqadvantage mass analyzer. Melting points were determined on a SGW X-4 microscopic melting point apparatus and are uncorrected.

**Preparation of $[Ni(HN_{Py}S_4)]_2{\cdot}MeOH$ (1a·MeOH)**

A 50 mL three-necked flask fitted with a magnetic stir-bar, two serum caps, and a $N_2$ inlet tube was charged with 1,2-benzenedithiol (0.285 g, 2.00 mmol) and a 1 M solution of MeOLi (4 mL, 4 mmol) in MeOH (5 mL). After the mixture was stirred at room temperature for 15 min, a solution of $Ni(OAc)_2{\cdot}4H_2O$ (0.249 g, 1.00 mmol) in MeOH (5 mL) was added and then the new mixture was stirred for 1 h to give a brown-red solution. To this solution was added a solution of

2,6-bis[(tosyloxy)methyl]pyridine (0.448 g, 1.00 mmol) in THF(10 mL) and then the mixture was stirred for 12 h. The resulting brown-yellow suspension was filtered to give a solid, which was washed with THF (10 mL) and MeOH (10 mL), and then dried in vacuo to afford **1a**·MeOH (0.336 g, 73%) as a brown solid, mp > 250 °C. Anal. Calcd for $C_{38}H_{30}N_2Ni_2S_8$·MeOH: C, 50.88; H, 3.72; N, 3.04. Found: C, 50.69; H, 3.92; N, 2.95. IR (KBr disk): 3052 (m, CH of aryl), 1593 (s), 1571 (s, CC of aryl), 739 (s, CH of aryl) $cm^{-1}$. MS (ESI, DMSO, $^{58}Ni$): m/z 885.7 [$M_{\mathbf{1a}}^+$].

**Preparation of [Ni(MeON$_{Py}$S$_4$)]$_2$·MeOH (1b·MeOH)**

The same procedure as that for preparation of **1a**·MeOH was followed, except that 2,6-bis[(tosyloxy)methyl]-4-methoxylpyridine (0.478 g, 1.00 mmol) was used instead of 2,6-bis[(tosyloxy)methyl]pyridine. **1b**·MeOH (0.313 g, 64%) was obtained as a brown solid, mp 180 °C (dec). Anal. Calcd for $C_{40}H_{34}N_2Ni_2O_2S_8$·MeOH: C, 50.22; H, 3.91; N, 2.86. Found: C, 49.80; H, 3.96; N, 2.61. IR (KBr disk): 3049 (m, CH of aryl), 1602 (s), 1567 (s, CC of aryl), 746 (s, CH of aryl) $cm^{-1}$. MS (ESI, DMSO, $^{58}Ni$): m/z 947.8 [$M_{\mathbf{1b}}^+$].

**Preparation of [Ni(ClN$_{Py}$S$_4$)]$_2$·MeOH (1c·MeOH)**

The same procedure as that for preparation of **1a**·MeOH was followed, except that 2,6-bis[(tosyloxy)methyl]-4-chloropyridine (0.482 g, 1.00 mmol) was utilized in place of 2,6-bis[(tosyloxy)methyl]pyridine. **1c**·MeOH (0.351 g, 71%) was produced as a brown solid, mp>250 °C. Anal. Calcd for $C_{38}H_{28}Cl_2N_2Ni_2S_8$·MeOH: C, 47.34; H, 3.26; N, 2.83. Found: C, 47.00; H, 3.56; N, 2.83. IR (KBr disk): 3042 (m, CH of aryl), 1582 (s), 1570 (s, CC of aryl), 736 (s, CH of aryl) $cm^{-1}$. MS (ESI, DMSO, $^{58}Ni$): m/z

956.7[$M_{\mathbf{1c}}^{+}$].

**Preparation of [Ni(Br$N_{Py}S_4$)]$_2$·MeOH (1d·MeOH)**

The same procedure as that for preparation of **1a**·MeOH was followed, except that 2,6-bis[(tosyloxy)methyl]-4-bromopyridine (0.526 g, 1.00 mmol) was utilized in place of 2,6-bis[(tosyloxy)methyl]pridine. **1d**·MeOH (0.340 g, 63%) was produced as a brown-yellow solid, mp>250 °C. Anal. Calcd for $C_{38}H_{28}Br_2N_2Ni_2S_8$·MeOH: C, 43.44; H, 2.99; N, 2.60. Found: C, 43.15; H, 3.22; N, 2.35. IR (KBr disk): 3040 (m, CH of aryl), 1569 (s, CC of aryl), 740 (s, CH of aryl) $cm^{-1}$. MS (ESI, DMSO, $^{58}$Ni): m/z 1045.6 [$M_{\mathbf{1d}}^{+}$].

**Preparation of [Ni(*i*-Pr$N_{Py}S_4$)]$_2$ (1e)**

To the same equipped 50 mL flask as mentioned above was charged with 1,2-benzenedithiol (0.285 g, 2.00 mmol) and a 1 M solution of MeOLi (4 mL, 4 mmol) in MeOH (5 mL). After the mixture was stirred at room temperature for 15 min, a solution of $Ni(OAc)_2·4H_2O$ (0.249 g, 1.00 mmol) in MeOH (5 mL) was added and then the new mixture was stirred for 1 h to give a brown-red solution. To this solution was added a solution of 2,6-bis[(tosyloxy)methyl]-4-*i*-propylpyridine (0.490 g, 1.00 mmol; for its preparation, see the Supporting Information) in THF (5 mL) and then the mixture was stirred for 5 h to give a yellow precipitate. The precipitate was washed with MeOH (10 mL) and $Et_2O$ (10 mL) and then it was dissolved in $CH_2Cl_2$ (10 mL). After removal of the insoluble residue from $CH_2Cl_2$ by filtration, the filtrate was evaporated at reduced pressure to dryness. The resulting solid was further recrystallized in $CH_2Cl_2$/hexane (v/v = 1:4) at 5 °C to afford **1e** without MeOH (0.200

g, 41%) a brown solid, mp 174° (dec). Anal. Calcd for $C_{44}H_{42}N_2Ni_2S_8$: C, 54.33; H, 4.35; N, 2.88. Found: C, 54.26; H, 4.51; N, 2.88. IR (KBr disk): 3041 (m, CH of aryl), 1609 (s), 1555 (s, CC of aryl), 739 (s, CH of aryl) $cm^{-1}$. MS (ESI, DMSO, $^{58}Ni$): m/z 971.9 [$M_{\mathbf{1e}}^+$]. $\mu_{eff}$ (290 K) = 2.84 $\mu_B$.

**Preparation of $NiFe_2(HN_{Py}S_4)(CO)_5$ (2a) and $Fe(HN_{Py}S_4)(CO)$ (3a)**

A 50 mL three-necked flask equipped with a magnetic stir-bar, a serum cap, a $N_2$ inlet tube, and a reflux condenser topped with a $N_2$ outlet tube was charged with **1a**·MeOH (0.183 g, 0.20 mmol), $Fe_3(CO)_{12}$ (0.201 g, 0.40 mmol) and $CH_2Cl_2$ (10 mL). The mixture as a suspension was stirred and refluxed for 16 h and then cooled to room temperature. After solvent was removed at reduced pressure, the residue was subjected to flash column chromatography under anaerobic conditions. First, $CH_2Cl_2$/petroleum ether (v/v = 1:4) eluted a dark green band from which a small quantity of the unreacted $Fe_3(CO)_{12}$ was recovered. Subsequently, $CH_2Cl_2$ eluted a brown-red band from which **2a** (64 mg, 23%) was obtained as a brown-red solid. Finally, $CH_2Cl_2$/acetone (v/v = 4:1) eluted a red band from which **3a**[54] (0.077 g, 41%) was obtained as a red solid. **2a**, mp 180 °C (dec). Anal. Calcd for $C_{24}H_{15}Fe_2NNiO_5S_4$: C, 41.41; H, 2.17; N, 2.01. Found: C, 41.70; H, 2.17; N, 2.03. IR (KBr disk): $\nu_{C\equiv O}$ 1998 (vs), 1948 (s), 1921 (s) $cm^{-1}$. $^1H$ NMR (400 MHz, $d_6$-acetone): 4.55, 4.80 (dd, AX system, $J$ = 13.0 Hz, 2H, $NiSCH_2$), 4.94, 5.08 (dd, AB system, $J$ = 18.0 Hz, 2H, $FeSCH_2$), 7.01−7.50 (m, 8H, $2C_6H_4$), 7.98−8.05 (m, 3H, $C_5H_3N$) ppm. $^{13}C\{^1H\}$ NMR (100 MHz, $d_6$-acetone): 51.2, 51.4 ($CH_2$), 121.9, 126.4, 127.2, 127.3, 129.2, 130.0, 130.5, 131.9, 132.7, 133.3, 133.4, 134.6, 138.4, 150.1, 154.1, 156.9 ($2C_6H_4$, $C_5H_3N$),

212.0, 217.5, 222.4 (C≡O) ppm. **3a**, mp 208 °C (dec). Anal. Calcd for $C_{20}H_{15}FeNOS_4$: C, 51.17; H, 3.22; N, 2.98. Found: C, 51.09; H, 3.25; N, 2.71. IR (KBr disk): $\nu_{C\equiv O}$ 1957 (vs) $cm^{-1}$. $^1H$ NMR (400 MHz, $d_6$-acetone): 4.90, 5.02 (dd, AB system, $J$ = 16.8 Hz, 4H, $2CH_2$), 6.92–7.51 (m, 8H, $2C_6H_4$), 7.60–7.73 (m, 3H, $C_5H_3N$) ppm. $^{13}C\{^1H\}$ NMR (100 MHz, $d_6$-acetone): 56.8 ($CH_2$), 122.6, 123.1, 129.5, 131.1, 132.9, 133.8, 137.3, 158.5, 158.9 ($2C_6H_4$, $C_5H_3N$), 218.5 (C≡O) ppm.

**Preparation of $NiFe_2(MeON_{Py}S_4)(CO)_5$ (2b) and $Fe(MeON_{Py}S_4)(CO)$ (3b)**

A 50 mL three-necked flask equipped with a magnetic stir-bar, two serum caps, and a $N_2$ inlet tube was charged with **1b**·MeOH (0.196 g, 0.20 mmol), $Fe_3(CO)_{12}$ (0.202 g, 0.40 mmol), and $CH_2Cl_2$ (10 mL). After the suspended mixture was stirred at room temperature for 12 h, solvent was removed at reduced pressure to leave a residue. The residue was subjected to the same workup as that for preparation of **2a** and **3a** to afford **2b** (0.080 g, 28%) a brown-red solid and **3b** (0.105 g, 53%) as a red solid. **2b**, mp 140 °C (dec). Anal. Calcd for $C_{25}H_{17}Fe_2NNiO_6S_4$: C, 41.36; H, 2.36; N, 1.93. Found: C, 41.30; H, 2.56; N, 2.18. IR (KBr disk): $\nu_{C\equiv O}$ 1997 (vs), 1947 (vs), 1920 (s) $cm^{-1}$. $^1H$ NMR (400 MHz, $d_6$-acetone): 3.70 (s, 3H, $OCH_3$), 4.46, 4.70 (dd, AX system, $J$ = 12.8 Hz, 2H, $NiSCH_2$), 4.83, 4.94 (dd, AB system, $J$ = 18.0 Hz, 2H, $FeSCH_2$), 6.72–7.99 (m, 8H, $2C_6H_4$), 8.02, 8.04 (2s, 2H, $C_5H_2N$) ppm. $^{13}C\{^1H\}$ NMR (100 MHz, $d_6$-acetone): 52.0, 52.2 ($CH_2$), 56.6 ($OCH_3$), 108.3, 114.9, 127.2, 128.0, 130.0, 130.9, 131.5, 132.8, 133.7, 134.2, 134.3, 135.4, 151.1, 155.8, 158.9, 159.2, 167.7 ($2C_6H_4$, $C_5H_2N$), 212.8, 218.5, 223.4 (C≡O) ppm. **3b**, mp 176 °C (dec). Anal. Calcd for $C_{21}H_{17}FeNO_2S_4$: C, 50.50; H, 3.43; N, 2.80. Found: C, 50.45; H, 3.66; N,

2.84. IR (KBr disk): $\nu_{C\equiv O}$ 1961 (vs) $cm^{-1}$. $^{1}H$ NMR (400 MHz, $d_6$-acetone): 3.81 (s, 3H, $OCH_3$), 4.77, 4.95 (dd, AB system, $J$ = 17.0 Hz, 4H, $2CH_2$), 6.95–7.38 (m, 8H, $2C_6H_4$), 7.69–7.72 (m, 2H, $C_5H_2N$) ppm. $^{13}C\{^{1}H\}$ NMR (100 MHz, $d_6$-acetone): 56.0 ($CH_3$), 56.2 ($CH_2$), 108.1, 122.5, 128.8, 130.8, 131.6, 132.9, 156.9, 158.6, 165.5 ($2C_6H_4$, $C_5H_2N$), 215.8 (C≡O) ppm.

**Preparation of $NiFe_2(ClN_{Py}S_4)(CO)_5$ (2c) and $Fe(ClN_{Py}S_4)(CO)$ (3c)**

The same procedure as that for preparation of **2b** and **3b** was followed, except that **1c**·MeOH (0.198 g, 0.20 mmol) was employed instead of **1b**·MeOH and the mixture was stirred at room temperature for 18 h. **2c** (0.044 g, 15%) as a brown-red solid and **3c** (0.071 g, 35%) as a red solid were obtained. **2c**, mp 130 °C (dec). Anal. Calcd for $C_{24}H_{14}ClFe_2NNiO_5S_4$: C, 39.46; H, 1.93; N, 1.92. Found: C, 39.65; H, 2.15; N, 2.24. IR (KBr disk): $\nu_{C\equiv O}$ 2047 (m), 1996 (vs), 1952 (vs), 1910 (s), 1888 (s) $cm^{-1}$. $^{1}H$ NMR (400 MHz, $d_6$-acetone): 4.50, 4.82 (dd, AX system, $J$ = 12.8 Hz, 2H, $NiSCH_2$), 4.98, 5.06 (dd, AB system, $J$ = 18.0 Hz, 2H, $FeSCH_2$), 7.06–7.99 (m, 8H, $2C_6H_4$), 8.01–8.06 (m, 2H, $C_5H_2N$) ppm. $^{13}C\{^{1}H\}$ NMR (100 MHz, $d_6$-acetone): 51.8, 52.0 ($CH_2$), 122.9, 127.4, 128.1, 128.2, 130.2, 131.1, 131.6, 132.8, 133.7, 134.1, 134.3, 135.3, 146.0, 150.9, 156.3, 158.7, 159.4 ($2C_6H_4$, $C_5H_2N$), 212.9, 218.1, 223.1 (C≡O) ppm. **3c**, mp 140 °C (dec). Anal. Calcd for $C_{20}H_{14}ClFeNOS_4$: C, 47.67; H, 2.80; N, 2.78. Found: C, 47.90; H, 2.79; N, 2.49. IR (KBr disk): $\nu_{C\equiv O}$ 1968 (vs) $cm^{-1}$. $^{1}H$ NMR (400 MHz, $d_6$-acetone): 4.90, 5.02 (dd, AB system, $J$ = 16.8 Hz, 4H, $2CH_2$), 6.96–7.62 (m, 8H, $2C_6H_4$), 7.71–7.74 (m, 2H, $C_5H_2N$) ppm. $^{13}C\{^{1}H\}$ NMR (100 MHz, $d_6$-acetone): 56.5 ($CH_2$), 122.9, 123.3, 129.7, 131.1, 132.9, 133.6, 144.8, 158.3, 160.6

($2C_6H_4$, $C_5H_2N$), 218.3 (C≡O) ppm.

**Preparation of $NiFe_2(BrN_{Py}S_4)(CO)_5$ (2d) and $Fe(BrN_{Py}S_4)(CO)$ (3d)**

The same procedure as that for preparation of **2b** and **3b** was followed, except that **1d**·MeOH (0.216 g, 0.20 mmol) was used in place of **1b**·MeOH and the mixture was stirred at room temperature for 18 h. A small quantity of the unreacted $Fe_3(CO)_{12}$ was eluted by using $CH_2Cl_2$/petroleum ether (v/v = 1:4), **2d** (0.050 g, 16%) by using $CH_2Cl_2$, and **3d** (0.054 g, 25%) by using $CH_2Cl_2$/acetone (v/v = 20:1). **2d** is a brown-red solid, mp 126 °C (dec). Anal. Calcd for $C_{24}H_{14}BrFe_2NNiO_5S_4$: C, 37.20; H, 1.82; N, 1.81. Found: C, 37.09; H, 2.00; N, 1.64. IR (KBr disk): $\nu_{C\equiv O}$ 1992 (vs), 1950 (vs), 1907 (s), 1885 (s), 1843 (m) $cm^{-1}$. $^1H$ NMR (400 MHz, $d_6$-acetone): 4.50, 4.79 (dd, AX system, $J$ = 13.2 Hz, 2H, $NiSCH_2$), 4.98, 5.05 (dd, AB system, $J$ = 18.4 Hz, 2H, $FeSCH_2$), 7.08–8.01 (m, 8H, $2C_6H_4$), 8.02–8.06 (m, 2H, $C_5H_2N$) ppm. $^{13}C\{^1H\}$ NMR (100 MHz, $d_6$-acetone): 51.8, 52.0 ($CH_2$), 123.3, 126.1, 127.5, 128.3, 130.3, 131.1, 131.2, 131.7, 132.9, 133.8, 134.4, 134.9, 135.4, 151.0, 156.0, 158.8, 159.2 ($2C_6H_4$, $C_5H_2N$), 213.0, 218.2, 223.2 (C≡O) ppm. **3d** is a red solid, mp 142 °C (dec). Anal. Calcd for $C_{20}H_{14}BrFeNOS_4$: C, 43.81; H, 2.57; N, 2.55. Found: C, 43.59; H, 2.75; N, 2.59. IR (KBr disk):$\nu_{C\equiv O}$ 1967 (vs) $cm^{-1}$. $^1H$ NMR (400 MHz, $d_6$-acetone): 4.89, 5.01 (dd, AB system, $J$ = 17.0 Hz, 4H, $2CH_2$), 6.96–7.72 (m, 8H, $2C_6H_4$), 7.73–7.76 (m, 2H, $C_5H_2N$) ppm. $^{13}C\{^1H\}$ NMR (100 MHz, $d_6$-acetone): 56.4 ($CH_2$), 123.3, 126.0, 129.7, 131.2, 133.0, 133.5, 133.6, 158.3, 160.5 ($2C_6H_4$, $C_5H_2N$), 218.3 (C≡O) ppm.

**Preparation of $NiFe_2(i\text{-}PrN_{Py}S_4)(CO)_5$ (2e) and $Fe(i\text{-}PrN_{Py}S_4)(CO)$ (3e)**

A dark green solution of **1e** (0.195 g, 0.20 mmol) and $Fe_3(CO)_{12}$ (0.202 g, 0.40 mmol) in 10 mL of $CH_2Cl_2$ was stirred at room pemperature for 2 h until the solution color turned to deep brown. After solvent was removed at reduced pressure, the residue was subjected to flash column chromatography under anaerobic condictions. A dark green band was first eluted by using $CH_2Cl_2$/haxane (v/v = 1:4) from which a small quantity of unreacted $Fe_3(CO)_{12}$ was recovered. Then, $CH_2Cl_2$/hexane (v/v = 2:1) eluted the second brown-red band from which **2e** (0.053 g, 18%) was obtained as a brown-red solid. Finally, $CH_2Cl_2$ eluted a red band from which **3e** (0.035 g, 17%) was obtained as a red solid. **2e**, mp 106 °C (dec). Anal. Calcd for $C_{27}H_{21}Fe_2NNiO_5S_4$: C, 43.94; H, 2.87; N, 1.90. Found: C, 44.10; H, 2.94; N, 2.13. IR (KBr disk): $\nu_{C\equiv O}$ 2044 (m), 1999 (vs), 1948 (vs), 1921 (s) $cm^{-1}$. $^1H$ NMR (400 MHz, $d_6$-acetone): 0.98 (d, $J$ = 6.8 Hz, 6H, $CH(CH_3)_2$), 2.60–2.67 (m, 1H, $CH(CH_3)_2$), 4.50, 4.71 (dd, AX system, $J$ = 12.6 Hz, 2H, $NiSCH_2$), 4.92, 5.02 (dd, AB system, $J$ = 18.0 Hz, 2H, $FeSCH_2$), 6.98–7.99 (m, 8H, $2C_6H_4$), 8.03–8.06 (m, 2H, $C_5H_2N$) ppm. $^{13}C\{^1H\}$ NMR (100 MHz, $d_6$-acetone): 22.5, 22.9, 33.9 ($CH(CH_3)_2$), 52.3, 52.4 ($CH_2$), 120.6, 122.9, 126.8, 127.2, 128.1, 130.0, 130.8, 131.5, 132.8, 133.9, 134.2, 135.6, 150.9, 154.2, 157.6, 158.8, 161.5 ($2C_6H_4$, $C_5H_2N$), 212.9, 218.4, 223.5 (C≡O) ppm. **3e**, mp 89–91 °C. Anal. Calcd for $C_{23}H_{21}FeNOS_4$: C, 54.00; H, 4.14; N, 2.74. Found: C, 54.30; H, 4.22; N, 2.88. IR (KBr disk):$\nu_{C\equiv O}$ 1965 (vs) $cm^{-1}$. $^1H$ NMR (400 MHz, $d_6$-acetone): 1.08 (d, $J$ = 6.4 Hz, 6H, $CH(CH_3)_2$), 2.79–2.87 (m, 1H, $CH(CH_3)_2$), 4.84, 4.96 (dd, AB system, $J$ = 16.8 Hz, 4H, $2CH_2$), 6.93–7.40 (m, 8H, $2C_6H_4$), 7.70–7.73 (m, 2H, $C_5H_2N$) ppm. $^{13}C\{^1H\}$ NMR (100 MHz, $d_6$-acetone): 22.7, 22.9, 33.8 ($CH(CH_3)_2$), 56.6 ($CH_2$),

120.8, 122.9, 129.4, 131.0, 132.8, 133.8, 158.3, 158.5, 159.0 ($2C_6H_4$, $C_5H_2N$), 218.3 (C≡O) ppm.

**X-ray structure determinations of 1e, 2a/2b, and 3b/3c**

Single crystals suitable for X-ray diffraction analyses were grown by slow evaporation of the $CH_2Cl_2$/hexane solutions of **1e** at 25 °C, **2a/2b** at −5 °C, and **3b/3c** at −5 °C. All single crystals were mounted on a Rigaku MM-007 (rotating anode) diffractometer equipped with a Saturn 70 CCD or a Saturn 724 CCD. Data were collected at room temperature, using a confocal monochromator with Mo-Kα radiation (λ = 0.71073 or 0.71075 Å) in the $\omega$-$\phi$ scanning mode. Data collection, reduction and absorption correction were performed by CRYSTALCLEAR program.[71]The structures were solved by direct methods using the SHELXS-97 program[72] and refined by full-matrix least-squares techniques (SHELXL-97)[73] on $F^2$. Hydrogen atoms were located by using the geometric method. Details of crystal data, data collections and structure refinements are summarized in Tables 6 and 7.

**Table 6** Crystal data and structural refinement details for **1e, 2a** and **2b**

| | **1e** | **2a** | **2b** |
|---|---|---|---|
| Formula | $C_{44}H_{42}N_2Ni_2S_8$ ·$2CH_2Cl_2$ | $C_{24}H_{15}Fe_2NNiO_5S_4$ | $C_{25}H_{17}Fe_2NNiO_6S_4$ ·$CH_2Cl_2$ |
| $M_w$ | 1142.55 | 696.02 | 810.97 |
| Cryst syst | Tetragonal | Monoclinic | Monoclinic |
| Space group | P4(2)/n | P2(1)/c | Pc |
| $a$ (Å) | 20.917(3) | 14.660(3) | 10.806(4) |
| $b$ (Å) | 20.917(3) | 14.108(3) | 9.836(4) |
| $c$ (Å) | 11.136(2) | 14.217(3) | 14.282(5) |
| $\alpha$ (°) | 90 | 90 | 90 |
| $\beta$ (°) | 90 | 90.75(3) | 99.674(6) |
| $\gamma$ (°) | 90 | 90 | 90 |
| $V$ (Å$^3$) | 4872.2(14) | 2940.2(11) | 1496.5(10) |

| | | | |
|---|---|---|---|
| $Z$ | 4 | 4 | 2 |
| Crystal size/mm | 0.20 × 0.18 × 0.10 | 0.60 × 0.10 × 0.10 | 0.20 × 0.18 × 0.12 |
| $D_c$(g·cm$^{-3}$) | 1.558 | 1.572 | 1.800 |
| $\mu$ (mm$^{-1}$) | 1.371 | 1.924 | 2.080 |
| $F$(000) | 2352 | 1400 | 816 |
| Reflns collected | 48004 | 23189 | 18577 |
| Reflns unique | 4297 | 5179 | 6825 |
| $\theta_{min/max}$ (°) | 50.00 | 50.04 | 55.62 |
| Final $R$ | 0.0584 | 0.0849 | 0.0227 |
| Final $R_w$ | 0.1486 | 0.2312 | 0.0448 |
| GOF on F$^2$ | 1.101 | 1.082 | 0.993 |
| $\Delta\rho_{max/min}$/e Å$^{-3}$ | 0.892/-0.467 | 0.692/-0.625 | 0.341/-0.433 |

**Table 7** Crystal data and structure refinements details for **3b** and **3c**

| | **3b** | **3c** |
|---|---|---|
| Formula | $C_{21}H_{17}FeNO_2S_4$ | $C_{20}H_{14}ClFeNOS_4$ |
| $M_w$ | 499.45 | 503.86 |
| Cryst syst | Monoclinic | Monoclinic |
| Space group | P121/n1 | P2(1)/n |
| $a$ (Å) | 18.7900(13) | 8.1548(16) |
| $b$ (Å) | 10.9143(9) | 14.620(3) |
| $c$ (Å) | 20.023(2) | 16.658(3) |
| $\alpha$ (°) | 90 | 90 |
| $\beta$ (°) | 92.749(3) | 93.98(3) |
| $\gamma$ (°) | 90 | 90 |
| $V$ (Å$^3$) | 4101.6(6) | 1981.3(7) |
| $Z$ | 8 | 4 |
| Crystal size/mm | 0.24 × 0.22 × 0.20 | 0.20 × 0.18 × 0.12 |
| $D_c$(g·cm$^{-3}$) | 1.618 | 1.689 |
| $\mu$ (mm$^{-1}$) | 1.161 | 1.330 |
| $F$(000) | 2048 | 1024 |
| Reflns collected | 51207 | 20029 |
| Reflns unique | 9796 | 4709 |
| $\theta_{min/max}$ (°) | 55.84 | 55.72 |
| Final $R$ | 0.0279 | 0.0292 |
| Final $R_w$ | 0.0703 | 0.0732 |
| GOF on F$^2$ | 1.059 | 1.016 |
| $\Delta\rho_{max/min}$/e Å$^{-3}$ | 0.438/-0.427 | 0.365/-0.621 |

## Electrochemical and electrocatalytic experiments

Acetonitrile (HPLC grade) and dichloromethane (HPLC grade) were purchased from

Amethyst Chemicals. A solution of 0.1 M *n*-$Bu_4NPF_6$ in MeCN was used as electrolyte in each of the electrochemical and electrocatalytic experiments. *n*-$Bu_4NPF_6$ electrolyte was dried in an oven at 110 °C for at least 24 h. The electrolyte solutions were degassed by bubbling with $N_2$ for at least 10 min before measurements. The measurements were made using a BAS Epsilon potentiostat. All voltammograms were obtained in a three-electrode cell with a 3 mm diameter glassy carbon working electrode, a platinum counter electrode and an $Ag/Ag^+$ (0.01 M $AgNO_3$/0.1 M *n*-$Bu_4NPF_6$ in MeCN) reference electrode under an atmosphere of nitrogen. The working electrode was polished with 0.05 $\mu$m alumina paste and sonicated in water for about 10 min. BE experiments were run on a vitreous carbon rod ($A$ = 2.9 $cm^2$) in a two-compartment, gastight, H-type electrolysis cell containing ca. 25 mL of MeCN. All potentials are quoted against $Fc/Fc^+$ potential. Gas chromatography was performed with a Shimadzu gas chromatograph GC-2014 under isothermal conditions with nitrogen as a carrier gas and a thermal conductivity detector.

**Acknowledgements**

We are grateful to the Ministry of Science and Technology of China (973 programs 2011CB935902 and 2014CB845604) and the National Natural Science Foundation of China (21132001, 21272122, 21472095) for financial support of this work.

**References**

1 M. W. W. Adams and E. I. Stiefel, *Science*, 1998, **282**, 1842-1843.

2 R. Cammack, *Nature*,1999, **397**, 214-215.

3 R. K. Thauer, A. R. Klein and G. C. Hartmann, *Chem. Rev*., 1996, **96**, 3031-3042.

4 C. Tard and C. J. Pickett, *Chem. Rev.*, 2009, **109**, 2245-2274.

5 M. Frey, *ChemBioChem*, 2002, **3**,153-160.

6 Y. Nicolet, B. J. Lemon, J. C. Fontecilla-Camps and J. W. Peters, *Trends Biochem. Sci*., 2000, **25**, 138-143.

7 D. J. Evans and C. J. Pickett, *Chem. Soc. Rev.*, 2003, **32**, 268-275.

8 S. P. J. Albracht, *Biochim. Biophys. Acta*., 1994, **1188**, 167-204.

9 W. Lubitz, E. Reijerse and M. van Gastel, *Chem. Rev*., 2007, **107**, 4331-4365.

10 J. C. Fontecilla-Camps, A. Volbeda, C. Cavazza and Y. Nicolet, *Chem. Rev*., 2007, **107**, 4273-4303.

11 S. Shima and R. K. Thauer, *Chem. Rec*., 2007, **7**, 37-46.

12 S. Shima, O. Pilak, S. Vogt, M. Schick, M. S. Stagni, W. Meyer-Klaucke, E. Warkentin, R. K. Thauer and U. Ermler, *Science*, 2008, **321**, 572-575.

13 S. Dey, P. K. Das and A. Dey, *Coord. Chem. Rev*., 2013, **257**, 42-63.

14 H. Ogata, S. Hirota, A. Nakahara, H. Komori, N. Shibata, T. Kato, K. Kano and Y. Higuchi, *Structure*, 2005, **13**, 1635-1642.

15 A. Volbeda, E. Garcin, C. Piras, A. L. de Lacey, V. M. Fernandez, E. C. Hatchikian, M. Frey and J. C. Fontecilla-Camps, *J. Am. Chem. Soc*., 1996, **118**, 12989-12996.

16 Y. Higuchi, T. Yagi and N. Yasuoka, *Structure*, 1997, **5**, 1671-1680.

17 E. Garcin, X. Vernede, E. C. Hatchikian, A. Volbeda, M. Frey and J. C. Fontecilla-Camps, *Structure*, 1999, **7**, 557-566.

18 Y. Higuchi, H. Ogata, K. Miki, N. Yasuoka and T. Yagi, *Structure*, 1999, **7**, 549-556.

19 T. Hiromoto, E. Warkentin, J. Moll, U. Ermler and S. Shima, *Angew. Chem. Int. Ed.*, 2009, **48**, 6457-6460.

20 T. Hiromoto, K. Ataka, O. Pilak, S. Vogt, M. S. Stagni, W. Meyer-Klaucke, E. Warkentin, R. K. Thauer, S. Shima and U. Ermler, *FEBS Lett.*, 2009, **583**, 585-590.

21 W. Zhu, A. C. Marr, Q. Wang, F. Neese, D. J. E. Spencer, A. J. Blake, P. A.

Cooke, C. Wilson and M. Schröder, *Proc. Natl. Acad. Sci. U. S. A.*, 2005, **102**, 18280-18285.

22 F. Osterloh, W. Saak, D. Haase anf S. Pohl, *Chem.Commun*., 1997, 979-980.

23 C.-H. Lai, J. H. Reibenspies and M. Y. Darensbourg, *Angew. Chem. Int. Ed*., 1996, **35**, 2390-2393.

24 M. E. Carroll, B. E. Barton, D. L. Gray, A. E. Mack and T. B. Rauchfuss, *Inorg. Chem*., 2011, **50**, 9554-9563.

25 M. C. Smith, J. E. Barclay, S. P. Cramer, S. C. Davies, W.-W. Gu, D. L. Hughes, S. Longhurst and D. J. Evans, *Dalton Trans*., 2002, 2641-2647.

26 J. A. W. Verhagen, M. Lubitz, A. L. Spek and E. Bouwman, *Eur. J. Inorg. Chem*., 2003, 3968-3974.

27 J. Jiang, M. Maruani, J. Solaimanzadeh, W. Lo, S. A. Koch and M. Millar, *Inorg. Chem.*, 2009, **48**, 6359-6361.

28 B. E. Barton, C. M. Whaley, T. B. Rauchfuss and D. L. Gray, *J. Am. Chem. Soc*., 2009, **131**, 6942-6943.

29 D. Sellmann, F. Geipel, F. Lauderbach and F. W. Heinemann, *Angew. Chem. Int. Ed*., 2002, **41**, 632-634.

30 Q. Wang, J. E. Barclay, A. J. Blake, E. S. Davies, D. J. Evans, A. C. Marr, E. J. L. McInnes, J. McMaster, C. Wilson and M. Schröder, *Chem. Eur. J.*, 2004, **10**, 3384-3396.

31 S. Tanino, Z. Li, Y. Okhi and K. Tatsumi, *Inorg. Chem.*, 2009, **48**, 2358-2360.

32 Z. Li, Y. Ohki and K. Tatsumi, *J. Am. Chem. Soc.*, 2005, **127**, 8950-8951.

33 D. Sellmann, F. Lauderbach and F. W. Heinemann, *Eur. J. Inorg. Chem.*, 2005, 371-377.

34 S. Pal, Y. Ohki, T. Yoshikawa, K. Kuge and K. Tatsumi, *Chem. Asian J*., 2009, **4** , 961-968.

35 A. Perra, Q. Wang, A. J. Blake, E. S. Davies, J. McMaster, C. Wilson and M. Schröder, *Dalton Trans*., 2009, 925-931.

36 S. Canaguier, L. Vaccaro, V. Artero, R. Ostermann, J. Pécaut, M. J. Field and M. Fontecave, *Chem. Eur. J*., 2009, **15**, 9350-9364.

37 S. Ogo, K. Ichikawa, T. Kishima, T. Matsumoto, H. Nakai, K. Kusaka and T. Ohhara, *Science*, 2013, **339**, 682-684.

38 D. Schilter, T. B. Rauchfuss and M. Stein, *Inorg. Chem*., 2012, **51**, 8931-8941.

39 Y. Ohki, K. Yasumura, M. Ando, S. Shimokata and K. Tatsumi, *Proc. Natl. Acad. Sci. U. S. A*., 2010, **107**, 3994-3997.

40 S. Ogo, R. Kabe, K. Uehara, B. Kure, T. Nishimura, S. C. Menon, R. Harada, S. Fukuzumi, Y. Higuchi, T. Ohhara, T. Tamada and R. Kuroki, *Science*, 2007, **316**, 585-587.

41 L.-C. Song, J.-P. Li, Z.-J. Xie and H.-B. Song, *Inorg. Chem*., 2013, **52**, 11618-11626.

42 L.-C. Song, X.-J. Sun, P.-H. Zhao, J.-P. Li and H.-B. Song, *Dalton Trans*., 2012, **41**, 8941-8950.

43 Y. Guo, H. Wang, Y. Xiao, S. Vogt, R. K. Thauer, S. Shima, P. I. Volkers, T. B. Rauchfuss, V. Pelmenschikov, D. A. Case, E. E. Alp, W. Sturhahn, Y. Yoda and S. P. Cramer, *Inorg. Chem.*, 2008, **47**, 3969-3977.

44 X. Wang, Z. Li, X. Zeng, Q. Luo, D. J. Evans, C. J. Pickett and X. Liu, *Chem. Commun*., 2008, 3555-3557.

45 D. Chen, R. Scopelliti and X. Hu, *Angew. Chem. Int. Ed.*, 2011, **50**, 5671-5673.

46 A. M. Royer, T. B. Rauchfuss and D. L. Gray, *Organometallics*, 2009, **28**, 3618-3620.

47 A. M. Royer, M. Salomone-Stagni, T. B. Rauchfuss and W. Meyer-Klaucke, *J. Am. Chem. Soc.*, 2010, **132**, 16997-17003.

48 T. Liu, B. Li, C. V. Popescu, A. Bilko, L. M. Pérez, M. B. Hall and M. Y. Darensbourg, *Chem. Eur. J.*, 2010, **16**, 3083-3089.

49 L.-C. Song, G.-Y. Zhao, Z.-J. Xie and J.-W. Zhang, *Organometallics*, 2013, **32**, 2509-2512.

50 D. Chen, R. Scopelliti and X. Hu, *Angew. Chem. Int. Ed.*, 2012, **51**, 1919-1921.

51 L.-C. Song, F.-Q. Hu, M.-M. Wang, Z.-J. Xie, K.-K. Xu and H.-B. Song, *Dalton Trans*., 2014, **43**, 8062-8071.

52 L.-C. Song, Z.-J. Xie, M.-M. Wang, G.-Y. Zhao and H.-B. Song, *Inorg. Chem.*, 2012, **51**, 7466-7468.

53 B. Hu, D. Chen and X. Hu, *Chem. Eur. J.*, 2014, **20**, 1677-1682.

54 D. Sellmann, J. Utz and F. W. Heinemann, *Inorg.Chem.*, 1999, **38**, 5314-5322.

55 (a) D. F. Evans, *J. Chem. Soc.*, 1959, 2003-2005; (b) J. Löliger and R. Scheffold, *J. Chem. Edu.*, 1972, **49**, 646-647.

56 B. E. Barton and T. B. Rauchfuss, *J. Am. Chem. Soc.*, 2010, **132**, 14877-14885.

57 (a) M. Y. Darensbourg, I. Font, D. K. Mills, M. Pala and J. H. Reibenspies, *Inorg. Chem.*, 1992, **31**, 4965-4971; (b) B. Adhikary, S. Liu and C. R. Lucas, *Inorg. Chem.*, 1993, **32**, 5957-5962.

58 A. J. Bard and L. R. Faulkner, *Electrochemical Methods*, 2nd ed.; John Wiley & Sons, Inc.: New York, **2001**.

59 M. T. Olsen, A. K. Justice, F. Gloaguen, T. B. Rauchfuss and S. R. Wilson, *Inorg. Chem.*, 2008, **47**, 11816-11824.

60 A. Perra, E. S. Davies, J. R. Hyde, Q. Wang, J. McMaster and M. Schröder, *Chem. Commun.*, 2006, 1103–1105.

61 K. Weber, T. Krömer, H. S. Shafaat, T. Weyhermüller, E. Bill, M. van Gastel, F. Neese and W. Lubitz, *J. Am. Chem. Soc.*, 2012, **134**, 20745-20755.

62 G. A. N. Felton, R. S. Glass, D. L. Lichtenberger and D. H. Evans, *Inorg. Chem.*, 2006, **45**, 9181-9184.

63 D. Chong, I. P. Georgakaki, R. Mejia–Rodriguez, J. Sanabria–Chinchilla, M. P. Soriaga and M. Y. Darensbourg, *Dalton Trans.*, 2003, 4158-4163.

64 S. J. Borg, T. Behrsing, S. P. Best, M. Razavet, X. Liu and C. J. Pickett, *J. Am. Chem. Soc.*, 2004, **126**, 16988-16999.

65 (a) J.-F. Capon, F. Gloaguen, P. Schollhammer and J. Talarmin, *Coord. Chem. Rev.*, 2005, **249**, 1664-1676; (b) G. A. N. Felton, C. A. Mebi, B. J. Petro, A. K. Vannucci, D. H. Evans, R. S. Glass and D. L. Lichtenberger, *J. Organomet. Chem.*, 2009, **694**, 2681-2699.

66 P. J. Turrell, A. D. Hill, S. K. Ibrahim, J. A. Wright and C. J. Pickett, *Dalton Trans.*, 2013, **42**, 8140-8146.

67 S. Kaur-Ghumaan, L. Schwartz, R. Lomoth, M. Stein and S. Ott, *Angew. Chem. Int. Ed.*, 2010, **49**, 8033-8036.

68 D. M. Giolando and K. Kirschbaum, *Synthesis,*1992, **5**, 451-452 .

69 J. Kupai, P. Huszthy, K. Székely, T. Tóth and L. Párkányi, *ARKIVOC*, 2011 (ix) ,77-93.

70 R. B. King, *Organometallic Syntheses,* Academic Press: New York, 1965; Vol. 1, p 114; p 175.

71 *CrystalClear and CrystalStructure*, Rigaku and Rigaku Americas, The Woodlands, TX, **2007**.

72 G. M. Sheldrick, *SHELXS-97, Program for solution of crystal structures*, University of Göttingen, Germany, **1997**.

73 G. M. Sheldrick, *SHELXS-97, Program for refinement of crystal structures*, University of Göttingen, Germany, **1997**.

# The Graphical Contents Entry

## Novel reactions of homodinuclear $Ni_2$ complexes $[Ni(RN_{Py}S_4)]_2$ with $Fe_3(CO)_{12}$ to give heterotrinuclear $NiFe_2$ and mononuclear Fe complexes relevant to [NiFe]- and [Fe]-hydrogenases

**Li-Cheng Song,* Meng Cao and Yong-Xiang Wang**

The $[RN_{Py}S_4]$-type ligand-containing [NiFe]- and [Fe]-hydrogenase model complexes $NiFe_2(RN_{Py}S_4)(CO)_5$ (**2a-2e**) and $Fe(RN_{Py}S_4)(CO)$ (**3a-3e**) have been prepared by novel reactions of $Ni_2$ complexes $[Ni(RN_{Py}S_4)]_2$ (**1a-1e**) with $Fe_3(CO)_{12}$ under mild conditions. Complexes **2a–2e** and **3a–3e** have been found to be catalysts for proton reduction to hydrogen.